

ENTROPY ANALYSIS IN UNSTEADY MHD FLOW AND RADIATIVE HEAT TRANSFER
THROUGH POROUS MEDIUM ALONG A VERTICAL POROUS PLATE
IN THE PRESENCE OF VISCOUS DISSIPATION

POOJA SHARMA*¹, VIKAS KUMAR², AND KALPNA SHARMA³

^{1,3}Department of Mathematics & Statistics,
Manipal University Jaipur, Rajasthan, India-303007.

²Government Polytechnic College, Tonk - 304021, Rajasthan, India.

(Received On: 28-04-17; Revised & Accepted On: 26-05-17)

ABSTRACT

Effects of magnetic field, radiation on the entropy generation in unsteady flow of a viscous incompressible electrically conducting fluid through a porous medium along a vertical porous plate in the presence of viscous dissipation have been studied in the present paper. The nonlinear governing differential equations are solved numerically using Crank-Nicolson implicit finite difference method. Numerical results of; the velocity and temperature fields are utilized to compute the entropy generation number.

Keywords: Entropy generation; unsteady flow; MHD; radiation; porous medium; viscous dissipation.

NOMENCLATURE

B_0	Magnetic field intensity	σ	Electrical conductivity of the fluid
C_p	Specific heat of the fluid at constant pressure	u^*	velocity component along x* axis
Ec	Eckert number	u	Dimensionless velocity component along x axis
K^*	Permeability Parameter	U_0	Mean velocity of the plate
K	Dimensionless Permeability Parameter	v^*	Velocity component along y* axis
M	Hartmann number	v	Dimensionless velocity component along y axis
N	Radiation Parameter	V_0	The constant mean suction velocity
Pr	Prandtl number	κ	Thermal Conductivity
q_r^*	Heat flux per unit area	μ	Coefficient of Viscosity
t^*	Time	ν	Kinetic viscosity
t	Dimensionless time	θ	Dimensionless Temperature
T^*	Temperature of the fluid	ρ	Density of the fluid
T_∞	Temperature of the free Stream		

1. INTRODUCTION

In recent years, great price of energy and materials has controlled to a affected effort for searching more effectual and inexpensive heat interchange devices. In many engineering and manufacturing processes, entropy creation abolishes the available energy in the system. Therefore they are not able to exertion in their field as much they can, outstanding of the entropy generation. In last decays, this is a big problem that how to minimize the entropy generation for enhancing the optimal level of production. Many researchers are working to analyze the entropy generation process. Actually entropy exploration is a practice to enumerate the thermodynamic irreversibility which are conduction, convection and radiation in any fluid flow progression. This is also known as second law analysis and quite important because it is one of the methods used for predicting the performance of engineering processes. Clousius and Kelvin's studies on the irreversibility aspects of second law of thermodynamics are the base ground of the knowledge of entropy generation.

Corresponding Author: Pooja Sharma*¹,
¹Department of Mathematics & Statistics,
Manipal University Jaipur, Rajasthan, India-303007.

Many researchers have discussed and invented the theories based on these foundation. Bejan [1] studied the second law analysis in heat transfer and thermal design. Second law analysis of laminar viscous flow through a duct subjected to constant temperature was discussed by Sahin[2]. Nurusawa[3] investigated the second law analysis of mixed convection in rectangular ducts. Mahmud and Fraser[4] presented flow, thermal, and entropy generation characteristics inside a porous channel with viscous dissipation. Heat transfer to MHD oscillatory flow in a channel filled with porous medium was studied by Makinde and Mhone [5]. Hooman [6] investigated the entropy generation for microscale forced convection: effects of different thermal boundary conditions, velocity slip, temperature jump, viscous dissipation and duct geometry. Second law analysis for a variable viscosity plane Poiseuille flow with asymmetric convective cooling was discussed by Makinde and Aziz [7]. Thermodynamic second law analysis for a gravity driven variable viscosity liquid film along an inclined heated plate with convective cooling was studied by Makinde [8]. Cimpean and Pop [9] presented the parametric analysis of entropy generation in a channel filled with a porous medium. Unsteady hydromagnetic couette flow within a porous channel was studied by Seth *et al.* [10]. Chauhan and Kumar [11] investigated the radiation effects on unsteady flow through a porous medium channel with velocity and temperature slip boundary conditions. Eegunjobi and Makinde[12] presented the entropy generation analysis in a variable viscosity MHD channel flow with permeable walls and convective heating. Vyas and Rai [13] studied the entropy generation for radiative MHD Couette flow inside a channel with naturally permeable base. Recently Vyas and Srivastava [14] analyzed the entropy of generalized MHD couette flow inside a composite duct. Kumar *et al.* [15] discussed the entropy generation in poiseuille flow through a channel partially filled with a porous material.

Inspired by the above mentioned research work, we have made an attempt to analyze the second law of thermodynamics in unsteady MHD flow and radiative heat transfer through porous medium along a porous vertical non-conducting plate in the presence of viscous dissipation.

2. MATHEMATICAL FORMULATION

We consider the unsteady two-dimensional flow of a viscous incompressible electrically conducting fluid through a porous medium occupying semi-infinite region of space bounded by a vertical, infinite, porous, non-conducting plate in the presence of a uniform magnetic field applied normal to the direction of flow. Let x^* -axis be taken along the plate in upward direction and y^* -axis is taken normal to it, as shown in Figure 1.

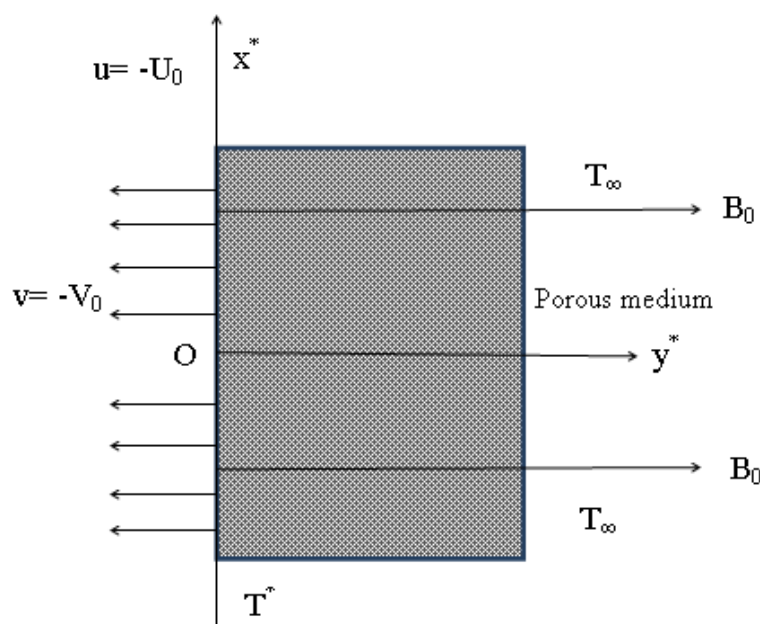


Figure-1: Physical model of the problem

The temperature in the fluid flowing is governed by the energy conservation equation involving radiative heat transfer. As the bounding surface is infinite in length, therefore all the physical variables of fluid are independent of x^* . By the usual boundary layer approximations, the governing equations of flow through porous medium [Darcy [16], Beavers and Beavers & Joseph. [17]] with Bousinesq approximation are :

Equation of continuity

$$(1) \quad \frac{\partial v^*}{\partial y^*} = 0 \Rightarrow v^* \text{ is independent of } y^* \Rightarrow v^* = -V_0 \text{ (constant).}$$

Equation of momentum

$$(2) \quad \frac{\partial u^*}{\partial t^*} - V_0 \frac{\partial u^*}{\partial y^*} = \nu \frac{\partial^2 u^*}{\partial y^{*2}} - \frac{\nu}{K^*} u^* - \frac{\sigma B_0^2}{\rho} u^* .$$

Equation of energy

$$(3) \quad \rho C_p \left\{ \frac{\partial T^*}{\partial t^*} - V_0 \frac{\partial T^*}{\partial y^*} \right\} = \kappa \frac{\partial^2 T^*}{\partial y^{*2}} + \mu \left(\frac{\partial u^*}{\partial y^*} \right)^2 + \sigma B_0^2 u^{*2} - \frac{\partial q_r^*}{\partial y^*} .$$

The initial and boundary conditions are

$$\text{For } t^* \leq 0; \quad u^* = 0, T^* = T_\infty, \quad \text{for all } y^* .$$

$$\text{For } t^* > 0; \quad u^* = U_0, \quad \frac{\partial T^*}{\partial y^*} = -\frac{q^*}{\kappa}, \quad \text{at } y^* = 0$$

$$u^* \rightarrow 0, \quad T^* \rightarrow T_\infty, \quad \text{as } y^* \rightarrow \infty ,$$

where all the physical quantities are defined in the nomenclature.

It is assumed that the medium is optically thin and with relatively low density. Following Cogley et al. [18] equilibrium model, we therefore take expression of radiative heat flux as follows

$$(5) \quad \frac{\partial q_r^*}{\partial y^*} = 4(T^* - T_\infty) \int_0^\infty K_{\lambda w} \left(\frac{\partial e_{b\lambda}}{\partial T} \right)_w d\lambda = 4I(T^* - T_\infty),$$

where $K_{\lambda w}$ is the absorption coefficient at the wall and $e_{b\lambda}$ is the plank constant.

3. METHOD OF SOLUTION

Introducing the following dimensionless quantities:

$$y = \frac{V_0 y^*}{\nu}, \quad u = \frac{u^*}{U_0}, \quad t = \frac{V_0^2 t^*}{\nu}, \quad \theta = \frac{T^* - T_\infty}{(q^* \nu / \kappa V_0)}, \quad Ec = \frac{U_0^2}{T_r C_p}, \quad K = \frac{V_0^2 K^*}{\nu^2}, \quad M = \frac{\sigma B_0^2 \nu}{V_0^2 \rho}, \quad Pr = \frac{\mu C_p}{\kappa},$$

$$(6) \quad N = \frac{4\nu I}{V_0^2 \rho C_p}, \quad T_r = \frac{q^* \nu}{\kappa V_0},$$

into the equations from (2) to (5), we get

$$(7) \quad \frac{\partial u}{\partial t} - \frac{\partial u}{\partial y} = \frac{\partial^2 u}{\partial y^2} - (K^{-1} + M)u,$$

$$(8) \quad Pr \left(\frac{\partial \theta}{\partial t} - \frac{\partial \theta}{\partial y} \right) = \frac{\partial^2 \theta}{\partial y^2} + Pr Ec \left(\frac{\partial u}{\partial y} \right)^2 + MEc Pr u^2 - N\theta,$$

The corresponding initial and boundary conditions in dimensionless form are

$$\text{For } t \leq 0; \quad u = 0, \theta = 0, \quad \text{for all } y^* .$$

$$\text{For } t > 0; \quad u = 1, \quad \frac{\partial \theta}{\partial y} = -1, \quad \text{at } y = 0$$

$$(9) \quad u \rightarrow 0, \quad \theta \rightarrow 0, \quad \text{as } y \rightarrow \infty ,$$

where all the physical quantities are defined in the nomenclature.

Now the differential equations (7) & (8) are second order partial differential equations. For solving these equations we have used the Crank-Nicolson implicit finite difference scheme.

4. NUMERICAL SOLUTION

The governing equations (7) and (8) subject to the initial and boundary conditions (9) are solved by Crank-Nicolson implicit finite difference scheme which is appropriate for the parabolic type of equation. The computational domain ($0 < t < \infty$) and ($0 < y < \infty$) are divided into a mesh of lines parallel to t and y axes.

By substituting the finite difference approximations to derivatives in equations (7) and (8), the governing equations are reduced to the following algebraic equations:

$$(10) \quad u_{i+1,j}[\lambda + \lambda\Delta y] - u_{i,j}[2\lambda + \lambda\Delta y + \Delta t(\frac{1}{K} + M) - 2] + u_{i-1,j}\lambda = \\ u_{i+1,j+1}(-\lambda - \lambda\Delta y) + u_{i,j+1}[2\lambda + \lambda\Delta y + \Delta t(\frac{1}{K} + M) + 2] - u_{i-1,j+1}\lambda.$$

$$(11) \quad [\lambda\Delta y Pr + \lambda]\theta_{i+1,j+1} - [\Delta y\lambda Pr + 2\lambda + NPr\Delta t + 2Pr]\theta_{i,j+1} + \lambda\theta_{i-1,j+1} = \\ -[\lambda + \lambda Pr\Delta y]\theta_{i+1,j} + [\lambda Pr\Delta y + 2\lambda + NPr\Delta t - 2Pr]\theta_{i,j} - \lambda\theta_{i-1,j} + R_{i,j} \text{ Where,}$$

$$R_{i,j} = -EcM\Delta t(u_{i,j}^2 + u_{i,j+1}^2)Pr - Ec\lambda Pr \left[(u_{i+1,j} - u_{i,j})^2 + (u_{i+1,j+1} - u_{i,j+1})^2 \right] \text{ and } \lambda = \frac{\Delta t}{(\Delta y)^2}, \quad \Delta t \text{ and}$$

Δy are mesh sizes.

In equations (10) and (11), the unknowns $u_{i,j+1}$ and $\theta_{i,j+1}$ are not expressed explicitly in terms of known quantities namely $u_{i-1,j}, u_{i,j}, u_{i+1,j}$ and $\theta_{i-1,j}, \theta_{i,j}, \theta_{i+1,j}$ at the time level j . The equation (10) and (11), written at all the interior mesh points form a tridiagonal system of linear algebraic equations, with the following initial and boundary conditions for velocity and temperature fields;

$$(12) \quad u_{i,1} = 0 \text{ and } \theta_{i,1} = 0, \quad i = 1, 2, 3, \dots, q+1$$

$$(13) \quad \left. \begin{aligned} u_{1,j} = 1, \quad u_{q+1,j} = 0 \\ \theta_{2,j} - \theta_{1,j} = -\Delta y, \quad \theta_{q+1,j} = 0 \end{aligned} \right\}, \quad j = 2, 3, 4, \dots, p+1$$

To find the numerical solution for the present problem, we divide the computational domains $0 < t < \infty$ and $0 < y < \infty$ into intervals with step sizes $\Delta t = 0.001$ and $\Delta y = 0.001$ for time t and space y , respectively. If we carry out the computations by changing step sizes slightly to check the stability of finite difference schemes, we observe that there is no significant change is seen in the results obtained by the numerical scheme. It is also known that implicit Crank-Nicolson scheme is convergent and stable for all values of λ .

5. RESULTS AND DISCUSSION

In the present paper the unsteady MHD flow and radiative heat transfer through porous medium along a vertical porous plate with dissipation effect is studied. The velocity, temperature and entropy analysis solutions are obtained by implicit Crank-Nicolson method. The effects of various parameters on the fluid velocity, temperature and entropy generation are shown through figures from (2) to (18).

It is observed from the figure (2) that fluid velocity is upsurging with the increase of permeability parameter (K) because the permeability of the porous medium helps the fluid flow. While the velocity of the fluid is falling with the rise in magnetic field parameter (M), due to the resistance created by Lorentz force to the flow. At the plate fluid is flowing with the plate velocity and gradually approaching to zero at far from the plate as under the boundary condition.

Figure 3 and 4 illustrate the effects of various parameters on temperature of the fluid. These figures display that the temperature of the fluid reduces with the rise in radiation parameter (N), permeability parameter (K), and Prandtl number (Pr); while raises with the increase of Eckert number (Ec) and magnetic field parameter (M). So, an increase in the fluid temperature is due to the presence of Ohmic heating (or Lorentz heating) which serves as additional heat source to the flow system.

6. ENTROPY GENERATION

In many engineering and industrial processes, entropy production destroys the available energy in the system. This is therefore imperative to determine the rate of entropy generation in a system, in order to optimize energy for efficient operation of the system.

The hydromagnetic boundary layer flow past a flat surface under the influence of thermal radiation and Newtonian heating is inherently irreversible. This is because of the exchange of energy and momentum, within the fluid and solid boundaries leading to continuous entropy generation [Bejan [19]]. Two major parts of entropy production can be identified. The first part is due to combined effects of heat transfer and thermal radiation in the direction of finite temperature gradients; while the other part due to the combined effects of fluid friction and joule heating. Hence the volumetric entropy generation in heat convection through a porous medium with the effect of magnetic field can be calculated by the following equation (Woods [20]):

$$(14) \quad E_G = \frac{\kappa}{T_r^2} \left(\frac{\partial T^*}{\partial y^*} \right)^2 + \frac{u}{T_r} \left(\frac{\partial u^*}{\partial y^*} \right)^2 + \frac{\sigma B_0^2}{T_r} u^{*2}.$$

In equation (14) the first term reflects the irreversibility because of the heat transfer and the mid-term is the entropy production outstanding of viscous dissipation. The third term is generated by the applied transverse magnetic field.

The dimensionless entropy generation number may be defined by the following correlation:

$$(15) \quad N_s = \frac{\nu^2}{\kappa V_0^2} E_G.$$

In terms of the dimensionless velocity and temperature the entropy generation number becomes

$$(16) \quad N_s = \left(\frac{\partial \theta}{\partial y} \right)^2 + EcPr \left(\frac{\partial u}{\partial y} \right)^2 + MEcPr u^2.$$

The entropy generation number N_s can be written as a summation of the entropy generation due to heat transfer denoted by N_1 and the entropy generation due to fluid friction and magnetic field denoted by N_2 given as

$$(17) \quad N_s = N_1 + N_2,$$

$$\text{where } N_1 = \left(\frac{\partial \theta}{\partial y} \right)^2; \quad N_2 = EcPr \left(\frac{\partial u}{\partial y} \right)^2 + MEcPr u^2.$$

The influences of the different governing parameters on entropy generation near the plate are presented in figures 5-18. It can be scrutinized from figures 5 and 6 that the entropy generation number N_s is increasing with the increase of Eckert number (Ec) while it is decreasing with the increase of permeability parameter (K). It is as expected as the fluid temperature is also increasing due to viscous dissipation and decreasing with permeability parameter. A perceptible behavior is observed in both the cases that entropy generation is increasing in the vicinity of the plate and then all of a sudden falling progressively far from the plate.

Figure 7 reveals the effect of radiation parameter on entropy generation. It shows that the entropy generation number is declining with the increase of thermal radiation parameter (N) due to the heat loss generated by radiation, as the same effect was observed on fluid temperature. From figure 8 and 9, it can be perceived that the entropy generation number N_s is growing with the increase of Prandtl number and intensity of the magnetic field. This promotion is more in the vicinity of the plate relatively far from the plate. A large variation of M causes a small variation in the rate of entropy generation. It can be seen that adjoining the plate once entropy increases and then get decrease distant from the plate for all values of Pr and M .

Figure 10-13 illustrate the effect of different governing parameter on entropy generation N_1 due to heat transfer. Figures 10 and 11 show that the entropy generation due to the heat transfer N_1 falls with the increase of radiative heat transfer parameter N Prandtl number Pr . At the plate entropy generation number N_1 due to heat transfer having a fixed value and then approaches to zero far from the plate as according to the boundary condition for all values of Pr and N .

From figure 12 and 13, we can observe the effect of magnetic field and Eckert number Ec on entropy generation N_1 due to heat transfer. It depicts that N_1 slightly increases with the large increase of magnetic field parameter (M). N_1 also raising with increasing values of Ec , likewise satisfying the boundary condition. But overall the effect of Ec and M is very small on Entropy generation N_1 due to heat transfer.

By figure 14 we can see entropy generation N_1 due to the heat transfer reduces with the increase of permeability parameter K . There is an interesting result obtained that for very less value of K , entropy generation N_1 due to the heat transfer is getting high value in the vicinity of the plate and then decreases suddenly throughout in the fluid far from the plate.

Figure 15-18 illustrate the effect of different governing parameter on entropy generation N_2 due to fluid friction and magnetic field. Figure 15 to 17 reveal that N_2 rises with the increase of Prandtl number (Pr), Eckert number Ec and Magnetic field parameter M . Near the plate Pr , Ec and M are more dominating in comparison of far from the plate.

The effect of permeability parameter K is depicted by figure 18. From this we can observe that due to the increase of K entropy generation N_2 due to fluid friction and magnetic field is growing. But Pr is not too much dominating in N_2 .

7. CONCLUSION

In the present study the effects of magnetic field and radiation on entropy generation in unsteady fully developed flow through porous medium along a vertical porous plate in the presence of viscous dissipation has been investigated. The velocity and temperature profiles are obtained by using the crank-Nicolson method. Their solutions are used to calculate the entropy generation. The effect of different parameters on velocity, temperature and entropy generation is scrutinized. Grounded on the received data analysis shown overhead, the subsequent deductions are concluded:

1. Velocity distribution is observed to rise with the growth of permeability parameter K whereas it shows the reverse effect in the case of magnetic field parameter M .
2. In the case of temperature distribution an increment is observed with viscous dissipation and magnetic field due to the presence of Ohmic heating. While contrary behavior is perceived with radiation parameter N , permeability parameter and prandtl number.
3. Combined entropy generation is getting more effected due to the fluid friction and magnetic field. An cumulative behavior is observed with an rise of Ec , Pr , and M . While reverse behavior is seen with increasing effect of K and N . Along with that in most of the cases, entropy is increasing near the plate and then decreasing behavior is shown throughout in the vicinity of the plate region.

REFERENCES

1. BEJAN, A. Second law analysis in heat transfer and thermal design. Ad. Heat Tans, 15(1982), 1-58.
2. SAHIN, A. Z. Second law analysis of laminar viscous flow through a duct subjected to constant temperature. J Heat Transfer, 120(1998), 76-83.
3. NARUSAWA, U. The second law analysis of mixed convection in rectangular ducts. Heat & Mass Transfer, 37(1998), 197-203.
4. MAHMUD, S., R. A. FRASER. Flow, thermal, and entropy generation characteristics inside a porous channel with viscous dissipation. International Journal Sciences, 44(1) (2005), 21-32.
5. MAKINDE, O. D., P.Y. MHONE. Heat transfer to MHD oscillatory flow in a channel filled with porous medium. Romanian Journal of Physics, 50(2005), 931-938.
6. HOOMAN, K. Entropy generation for microscale forced convection: effects of different thermal boundary conditions, velocity slip, temperature jump, viscous dissipation and duct geometry. International communication in Heat and Mass Transfer, 34 (8) (2007), 945-957.
7. MAKINDE, O. D., A. AZIZ. Second law analysis for a variable viscosity plane poiseuille flow with asymmetric convective cooling. Comput. Math. Appl., 60(2010), 3012-3019.
8. MAKINDE, O. D. Thermodynamic second law analysis for a gravity driven variable viscosity liquid film along an inclined heated plate with convective cooling. J. Mech. Sci. Technol., 24(2010), 899-908.
9. CIMPEAN, D., I. POP. Parametric analysis of entropy generation in a channel filled with a porous medium. Recent Researchers in applied and Computational Mathematics WSEAS ICACM (2011), 54-59.
10. SETH, G. S., M. S. ANSARI, R. NANDKEOLYAR. Unsteady hydromagnetic coquette flow within a porous channel. Tamkang Journal of Science and Engineering, 14(1) (2011), 7-14.
11. CHAUHAN, D. S., V. KUMAR. Radiation effects on unsteady flow through a porous medium channel with velocity temperature slip boundary condition. Appl. Mathematical Sciences, 6(2012), 1759-1769
12. EEGUNJOBI, A. S., O. D. MAKINDE. Entropy generation analysis in a variable viscosity MHD channel flow with permeable walls and convective heating. Mathematical Problems in Engineering, 2013(2013), 1-12.
13. VYAS, P., A. RAI. Entropy generation for radiative MHD couette flow inside a channel with naturally permeable base. Int. J. Energy Techno., 5(19) (2013), 1-9.
14. VYAS, P., N. SRIVASTAVA. Entropy Analysis of generalized MHD Couette flow inside a composite duct with asymmetric convective cooling. Arabian J. Sci. Eng., 40(2015), 603-614.
15. KUMAR V, S. JAIN, K. SHARMA, P. SHARMA. Entropy generation in poiseuille flow through a channel partially filled with a porous material. Theoretical and Applied Mechanics 42(2015),35-51
16. DARCY, H. The flow of fluids through porous media. Mc Graw-Hill Book Co New York, 1937.

17. BEAVERS, G. S., D. D. JOSEPH. Boundary conditions at a naturally permeable wall. J. Fluid Mech., 30 part 1 (1967),197-207.
18. COOGLEY, A. C. L, O. A. VINVENT AND E. S. GILES. Differential approximation for radiative hear transfer in non-linear equations-grey gas near equilibrium. American Institute of Aeronautics 6, 5(1968) 51-553.
19. BEJAN, A. Entropy Generation Minimization. CRC: Boca, Raton, FL, USA, 1996.
20. WOODS L. C. Thermodynamics of fluid systems. Oxford University Press, UK, (1975).

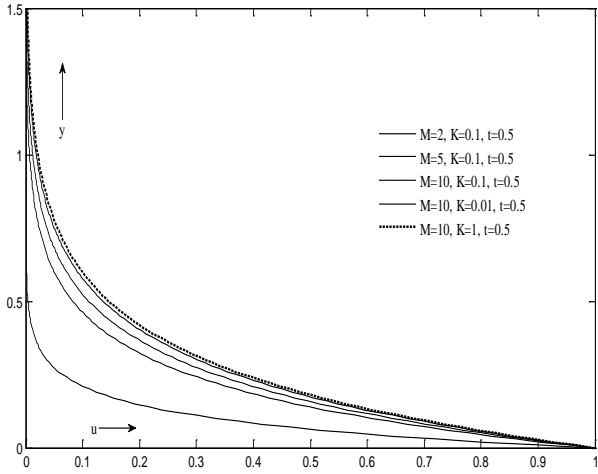


Fig. 2 Velocity Profiles versus y when $t=0.5$

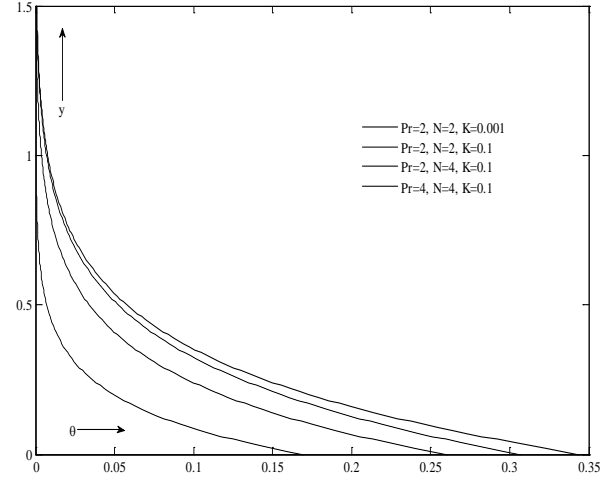


Fig. 3 Temperature versus y when $t = 0.5$, $Ec = 0.01$, $M = 2$.

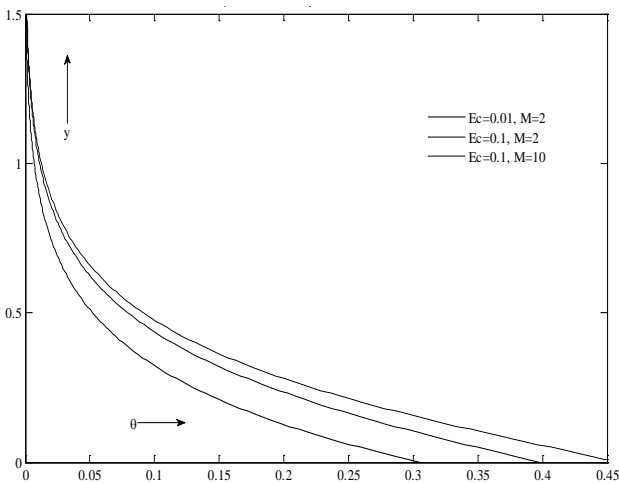


Fig. 4 Temperature versus y when $t = 0.5$, $N = 2$, $K = 0.1$, $Pr = 2$

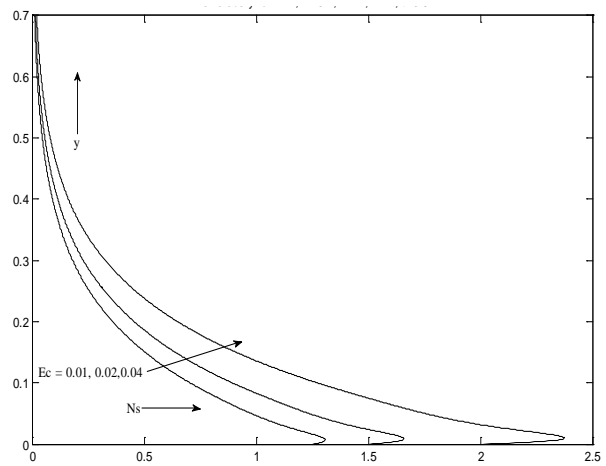


Fig. 5 Entropy Generation N_s versus y when $t = 0.5$, $N=2$, $K=0.1$, $Pr=2$, $M=2$.

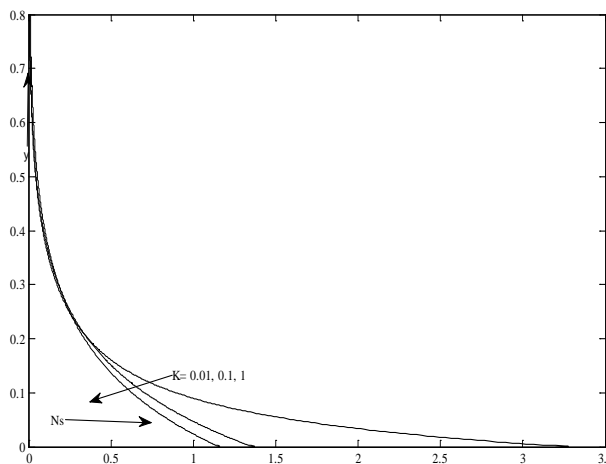


Fig. 6 Entropy Generation N_s versus y when $t=0.5$, $N=2$, $Pr=2$, $Ec=0.01$, $M=2$

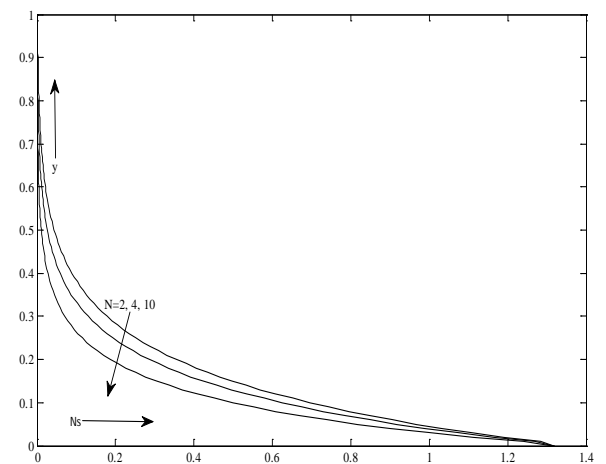


Fig. 7 Entropy Generation N_s versus y when $t=0.5$, $Pr=2$, $K=0.1$, $Ec=0.01$, $M=2$

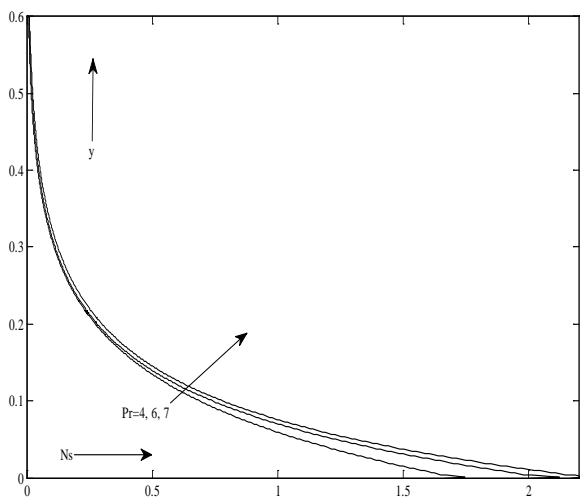


Fig. 8 Entropy Generation N_s versus y when $t=0.5$, $N=2$, $K=0.1$, $Ec=0.01$, $M=2$

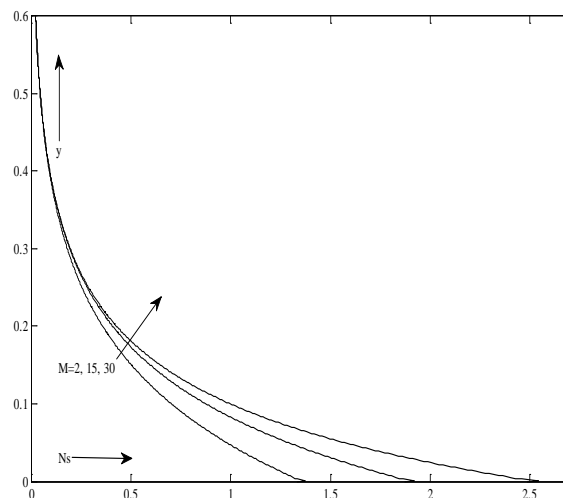


Fig. 9 Entropy Generation N_s versus y when $t=0.5$, $N=2$, $K=0.1$, $Ec=0.01$, $Pr=2$

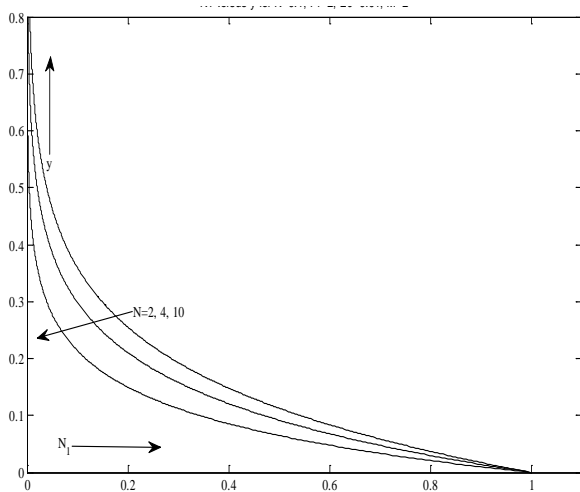


Fig. 10 Entropy Generation N_1 due to heat transfer versus y when $K=0.1$, $Pr=2$, $Ec=0.01$, $t=0.5$, $M=2$

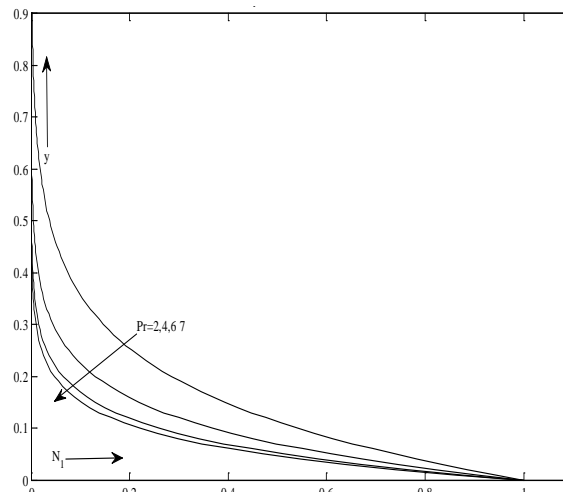


Fig. 11 Entropy Generation N_1 due to heat transfer versus y when $t=0.5$, $N=2$, $K=0.1$, $Ec=0.01$, $M=2$

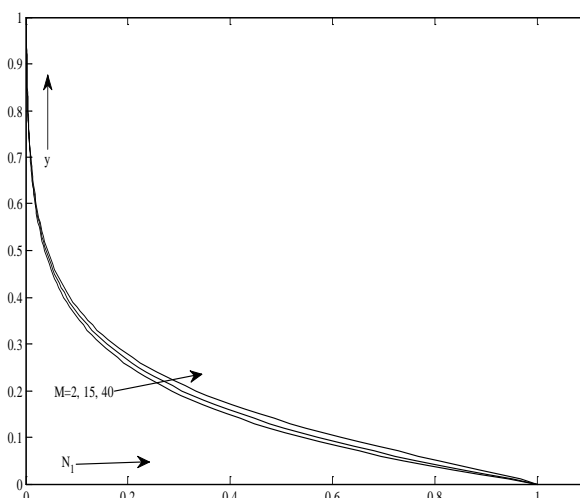


Fig. 12 Entropy Generation N_1 due to heat transfer versus y when $t=0.5$, $N=2$, $K=0.1$, $Pr=2$, $Ec=0.01$

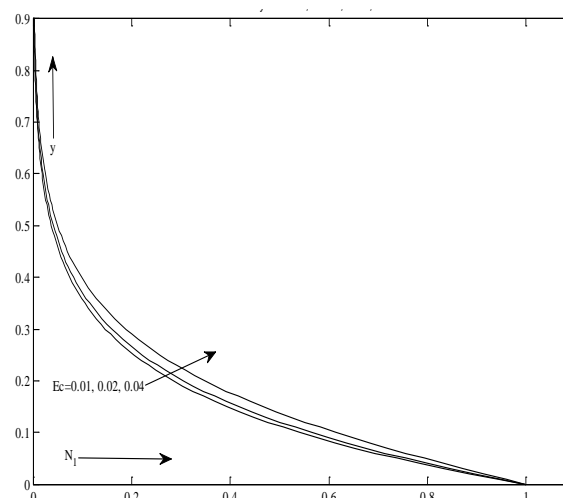


Fig. 13 Entropy Generation N_1 due to heat transfer versus y when $t=0.5$, $N=2$, $K=0.1$, $Pr=2$, $M=2$

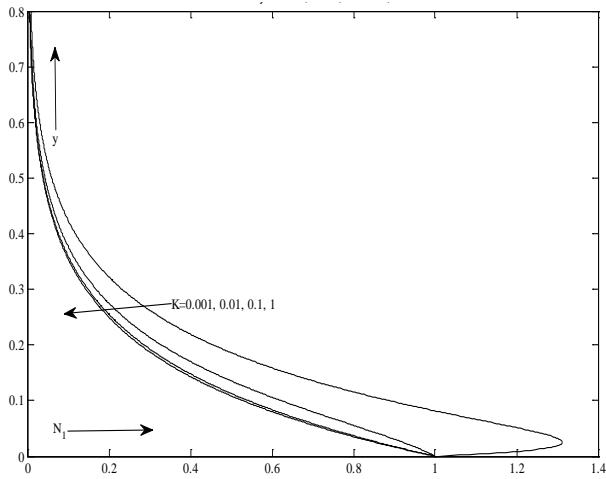


Fig. 14 Entropy Generation N_1 due to heat transfer versus y when $t=0.5$, $N=2$, $Ec=0.01$, $Pr=2$, $M=2$

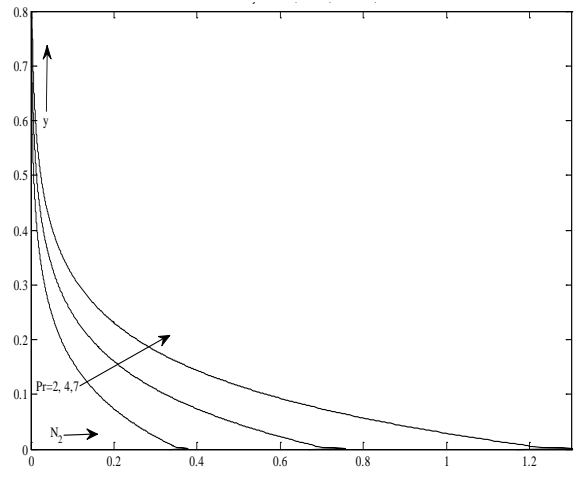


Fig. 15 Entropy Generation N_2 due to fluid friction with magnetic field, versus y when $t=0.5$, $N=2$, $Ec=0.01$, $K=0.1$, $M=2$

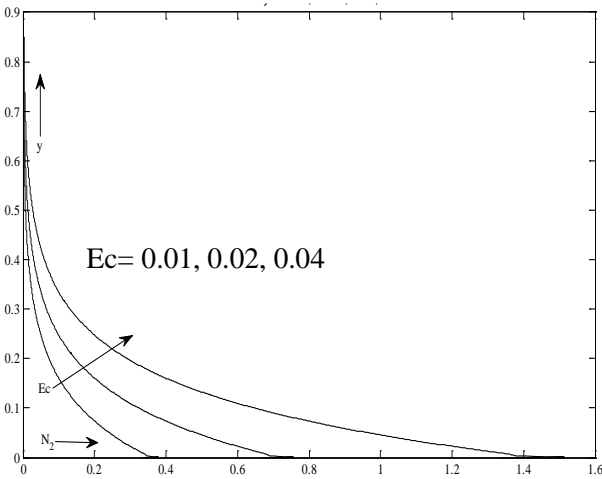


Fig. 16 Entropy Generation N_2 due to fluid friction with magnetic field, versus y when $t=0.5$, $N=2$, $K=0.1$, $Pr=2$, $M=2$

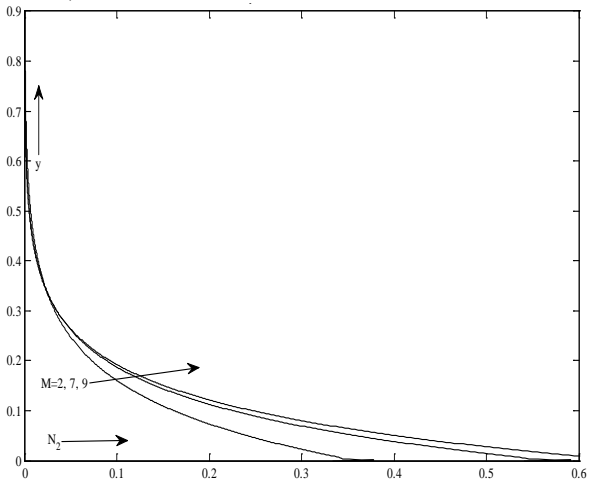


Fig. 17 Entropy Generation N_2 due to fluid friction with magnetic field, versus y when $t=0.5$, $N=2$, $K=0.1$, $Pr=2$, $Ec=0.01$

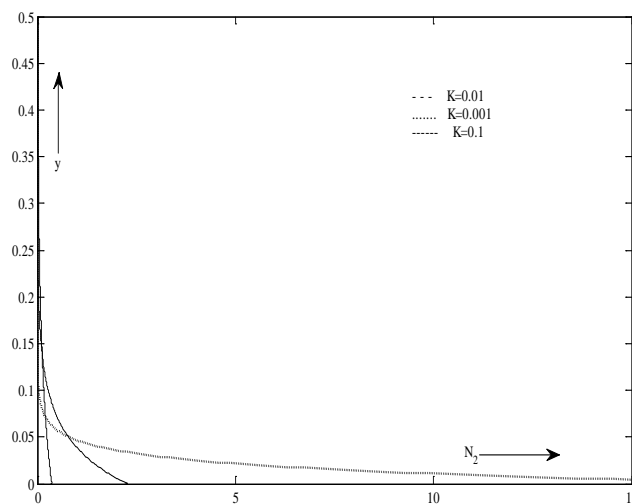


Fig. 18 Entropy Generation N_2 due to fluid friction with magnetic field versus y when $t=0.5$, $N=2$, $Ec=0.01$, $Pr=2$, $M=2$.

Source of support: Nil, Conflict of interest: None Declared.

[Copy right © 2017. This is an Open Access article distributed under the terms of the International Journal of Mathematical Archive (IJMA), which permits unrestricted use, distribution, and reproduction in any medium, provided the original work is properly cited.]